Applied Surface Science 383 (2016) 64–70

Contents lists available at ScienceDirect

Applied Surface Science

journal homepage: www.elsevier.com/locate/apsusc

New kinetic insight into the spontaneous oxidation process of lithium in air by EPMA

Manuel Otero[a,b], German Lener[c], Jorge Trincavelli[a,*], Daniel Barraco[a], Marcelo Sandro Nazzarro[c], Octavio Furlong[c], Ezequiel Pedro Marcos Leiva[b]

[a] IFEG, Facultad de Matemáticas, Astronomía y Física, Universidad Nacional de Córdoba, Córdoba, Argentina
[b] INFICQ, Departamento de Matemáticas y Física, Facultad de Ciencias Químicas, Universidad Nacional de Córdoba, Córdoba, Argentina
[c] INFAP, Facultad de Ciencias Físico Matemáticas y Naturales, Universidad Nacional de San Luis, San Luis, Argentina

ARTICLE INFO

Article history:
Received 1 February 2016
Received in revised form 7 April 2016
Accepted 8 April 2016
Available online 25 April 2016

Keywords:
Lithium corrosion
Electron Probe Micro-Analysis
Oxide growth kinetics

ABSTRACT

The exposure of metallic lithium to ambient air produces a fast corrosion reaction of the surface that continues to the bulk of the material. This spontaneous process was explored by means of X-ray Photoelectron Spectroscopy (XPS) and Electron Probe Micro-Analysis (EPMA). The combination of these techniques and Monte Carlo simulations allowed observing the formation of a film of lithium hydroxide (LiOH) and studying the growth within the material during the first 300 s. The corrosion is mainly due to the reaction of lithium with water and the diffusion of water through the growing LiOH film is the rate determining step. On the basis of a kinetic analysis we studied the mechanism of reaction and inferred a diffusion coefficient of $D = (5.1 \pm 0.4) \times 10^{-12}$ cm^2/s in agreement with results from the literature obtained using different techniques.

1. Introduction

Rechargeable lithium batteries have become of primary importance due to their technological application in portable electronic devices, and appear as the most promising alternative to drive transportation on the basis of sustainable electricity in the near future [1]. Currently, the market of rechargeable batteries is primarily based on Li-ion batteries and the production is continually increasing [2]. However, to extend their applicability for the future technology, their energy density and capacity must be improved. Several researchers focus on other types of batteries such as Li-air and Li-S, having potentially theoretical capacities 10 times higher and reduced prices. These batteries are based on the use of metallic Li as anode material. On these grounds, theoretical as well as experimental research on the materials involved in this kind of batteries is highly desirable. Li is an alkaline metal that reacts rapidly with humid air, and knowledge on the kinetics of this phenomenon may be relevant for the production and safety of these systems. It has been pointed out in a recent review [3], that although the studies on these systems date from decades, the mechanism and kinetics of the corrosion of metallic lithium and related compounds is still a topic of debate. In fact, a Scopus search shows that the publication rate is rather discontinuous and episodic.

Markowitz and Boryta [4] studied the corrosion of lithium metal by circulating air at 50% relative humidity into a 100–125-mesh metal dispersion prepared from pure bulk lithium metal. X-ray examination of a number of samples of this metal showed that products formed at the beginning of the corrosion process were mainly anhydrous lithium hydroxide and lithium nitride. Subsequently, anhydrous and hydrated lithium hydroxide were formed with a concomitant decrease of the lithium nitride. On the other hand according to Tipton [5], lithium metal develops a black nitride tarnish when exposed to air. This black tarnish has been observed in the present experiments after few minutes of exposure to air at atmospheric pressure, and room temperature and humidity. Nevertheless, this black film observed does not necessarily need to be lithium nitride [3]. Particularly, when exposed to pure O_2 and N_2, the reaction with the lithium surface was observed to occur more rapidly with O_2 than with N_2 [6]. In addition, no Li_3N was observed for lithium foils prepared by sputter-evaporation and exposed to air during 10 h [7].

In order to characterize the growth kinetics of the corrosion layer occurring when a Li surface is exposed to air under room conditions, the intensity of the oxygen Kα characteristic line in the X ray emission spectrum collected in a scanning electron microscope was measured for different exposure times of a Li foil to air. The

* Corresponding author.
E-mail address: trincavelli@famaf.unc.edu.ar (J. Trincavelli).

http://dx.doi.org/10.1016/j.apsusc.2016.04.060
0169-4332/

experimental results were interpreted with the aid of Monte Carlo simulations. This type of study is unprecedented in the literature.

2. Experimental procedure

2.1. Materials

Li foils were cut out of a Li ribbon (99.9%, ALDRICH 265993). Li manipulation was performed inside a glove box with controlled Ar atmosphere (<0.5 ppm of oxygen and water). The initial status of the Li foils was found to be critical for the present studies. For this reason, freshly cut foils were used for each experiment, as delivered from the provider. The Li samples were mounted onto sample holders for the scanning electron microscope (SEM) inside the glove box and placed inside a transport chamber filled with Ar prior to the air-exposure experiments. After a controlled exposure time to air, they were inserted in the SEM chamber. The temperature and air humidity in the measurement room were in the range of (296 ± 1) Kelvin and (50 ± 7)%, respectively.

2.2. EPMA-SEM

The Li foils were imaged in a SEM-FEG Zeiss instrument; model Sigma. To obtain the X-ray spectra, an energy dispersive spectrometer was used attached to the SEM, which consists of a silicon drift Oxford detector with an Aztec characterization system. The energy of the incoming electrons was $E_0 = 4$ keV.

2.3. X-ray photoelectron spectroscopy (XPS)

X-ray photoelectron spectra of the Li foils were collected using a VG Microtech ESCA spectrometer with a non-monochromatic Al Kα radiation source (300 W, 15 kV, $h\nu = 1486.6$ eV), combined with a VG-100-AX hemispherical analyzer operating at 25 eV pass energy. The instrumental resolution was 0.1 eV. All the XPS spectra were calibrated with a reference to the adventitious C1s peak at 284.8 eV, to rule out any possible spectral shift due to a charging effect. The chamber pressure was kept at $<10^{-9}$ Torr during the measurements.

3. Development of the measurement methodology

In spite of the discussion on the presence of Li_3N given in the introduction, the emission X-ray spectra registered in the present study (see Fig. 5 below) did not show the presence of N in the bulk samples prepared, which allows us to rule out the formation of lithium nitride (the nitrogen peak should be at 0.39 keV). Further X-ray photoelectron spectroscopy (XPS) measurements of the oxygen 1s peak were performed to corroborate that the specimen formed at the surface was lithium hydroxide. Fig. 1 shows the O 1s spectrum of a lithium surface exposed to air during 3 s and 5 min at atmospheric pressure. The same spectrum was observed for longer exposure times (up to 1 h), showing similar features (not shown in Fig. 1). The reference sample was made by exposition of a fresh Li foil to pure water, as performed by Hoenigman and Keil [8], to ensure the existence of both the oxide and hydroxide peaks. It is observed that in the studied samples no Li_2O is formed. Also no evidence for the presence of nitride was found in the XPS measurements. The formation of Li_2CO_3 has been reported in the case of Mg-Li alloys exposed to air [9,10]. According to Zeng et al. [9] this carbonate species should show a peak due to the C=O bond at 531.5 eV, which is not observed in our O1s XPS spectra.

The occurrence of Li_2O_2 can also be disregarded on the basis of our XPS results. According to the literature, the binding energy of the O1s peak for Li_2O_2 should occur at 531.5 eV [11,12]. In our measurements the O1s peak is located at 530.7 eV, that is, it is shifted towards considerably lower binding energies. According to these authors, this is an indication that "surface species with lower oxidation state, e.g. LiOH are formed". Furthermore, Tanaka et al. [13] assign the O1s XPS peak around 531 eV to LiOH, as the peak obtained in our measurements. Therefore, it can be considered that, under the experimental conditions used in this work, the layer formed on the metallic lithium tape is mainly composed of anhydrous lithium hydroxide.

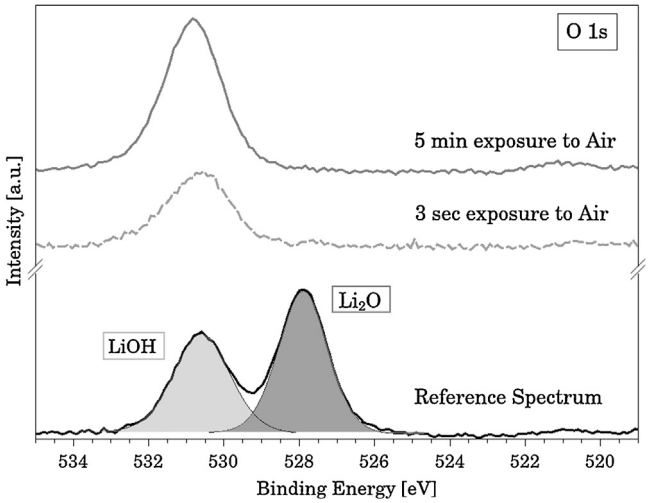

Fig 1. Oxygen 1 s XPS spectra of lithium exposed to air at atmospheric pressure during 3 s (dashed line) and during 5 min (solid line). A reference sample with LiOH and Li_2O peaks was also measured.

When a flat sample is irradiated with a high energy electron beam, the incident particles suffer several interactions with the atoms and they are usually stopped within the material, provided it is thick enough (*i.e.*, in the case of electrons with incidence energy E_0 lower than 10 keV, they run typically below one micrometer). Among the different interactions undergone by the electrons and the sample atoms, an inner shell ionization can be followed by a radiative decay. The number of characteristic X-ray photons produced after a particular decay is proportional to the concentration of the respective elements in the sample. In the configuration studied here, a nanometric film of LiOH was found to lay on the Li substrate, which can be considered to be semi-infinite. Bearing the previous ideas in mind, it can be stated that the thicker the hydroxide film, the more intense the O-Kα peak detected, at least within a certain thickness range. Moreover, it is reasonable to assume that in the thin film regime, the peak intensity I is proportional to the film mass thickness $\rho.x$, for layers of mass density ρ and linear thickness x, because for this case, self-absorption and electron scattering can be neglected [14]. For larger thicknesses, the slope of the I vs. x curve decreases until the hydroxide thickness equals the maximum penetration depth of electrons, where saturation takes place, since in this case the whole region of the material reached by the electron beam is within the hydroxide layer [15].

In order to find a convenient value for E_0, the relationship between I and x was analyzed by means of Monte Carlo simulations. To do that, the software package PENELOPE was used [16]. It must be taken into account that a high value of E_0 leads to a large interaction volume of the electrons in the material, *i.e.*, a region in the sample that could be too large as compared with the region of interest. The latter fact could mean a low sensitivity to analyze the relatively thin corrosion layers formed in few seconds. On the other hand, if E_0 is too low, saturation could be reached at a very low thickness, that is, very rapidly. After several Monte Carlo tests,

a value of 4 keV was found suitable for the time intervals where the most intense formation of LiOH takes place.

On the basis of the previous analysis, additional simulations were performed for incident electrons of 4 keV in kinetic energy, in a configuration considering an uniform LiOH layer on Li, assuming a mass density $\rho = 1.46\,g/cm^3$. The thicknesses considered, in nm, where: 1, 2, 4, 10, 20, 40,. . ., 400 and 600, where ". . ." denotes that intermediate values between 40 and 400 were taken in 20 nm steps. The characteristic O-Kα intensity values obtained for all these simulations are shown in Fig. 2.

As can be observed, after an approximately linear behavior for the lower thicknesses, the curve slope slightly increases and finally decreases down to zero after 300 nm. A hyperbolic tangent function:

$$I(x) = tanh\left[(Ax + B)^C\right] \quad (1)$$

was fitted to the simulated data, producing an excellent agreement for the fitting parameters $A = 0.0050$, $B = 0.050$ and $C = 1.49$, where x is expressed in nm.

The simulation results plotted in Fig. 2 suggest that the characteristic O-Kα intensity is a good indicator of the LiOH layer thickness, as long as it is below 300 nm for the incidence energy of 4 keV used. On the basis of this preparatory frame, spectra acquisition induced by 4 keV electrons impinging on a lithium tape was planned for the following times under air exposure: 7, 12, 20, 28, 37, 52, 67, 87, 107, 207, 307, 407, 507, 707 s. The minimum time required to move the sample from the transportation box to the SEM chamber was 6 s, where 1 s corresponds to the estimated elapsed time in contact with air, from the beginning of the chamber closing until air is almost fully evacuated. This short period was estimated taking into account that the SEM chamber is vented with gaseous nitrogen instead of air. Samples for the different exposure times were obtained by adding a new period in air to the previous ones. For each air-corroded sample, a SEM image was taken and five X-ray emission spectra were registered.

The value of the net peak intensity was determined following two steps. First, the background below the O-Kα peak, caused by bremsstrahlung, was subtracted. Then, the net intensity was normalized to account for any fluctuation in the electron beam current. To this purpose, the spectral background was integrated in the peak-free region between 1 and 2 keV. In this way, a possible variation in the beam current would affect similarly both peak and background, and thus would be cancelled out. However, bremsstrahlung depends on the sample mean atomic number, which certainly changes with the exposure time to air. This problem was addressed with the help of additional Monte Carlo simulations of the bremsstrahlung spectrum in the region of interest aiming to determine a correction coefficient for each normalization factor. These correction coefficients were calculated as the ratios between the integrated bremsstrahlung values corresponding to LiOH/Li samples and the integrated bremsstrahlung simulated for pure Li. Fig. 3 shows the results of these simulations. The correction coefficients vary from 1 (without LiOH layer) to 2 for LiOH layers above 300 nm.

4. Results and discussion

As mentioned in the previous section, a secondary electron image was taken for each exposure time. Fig. 4 shows four examples where the same sample region is recorded. The evident change in the surface morphology can be attributed to LiOH growth.

These changes are particularly noticeable along the material defects, showing that these sites are energetically favorable for the reaction that is taking place. As a second feature to observe, certain sparkles are increasingly visible for higher exposure times. This effect is characteristic of non-conductive samples, which remain locally charged under electron irradiation. In fact, the thin LiOH layer formed on the metallic lithium produces an increase in the surface electrical resistance that in sufficient to exhibit brighter images, but not as important to modify the Duane-Hunt limit in the X-ray spectra, which were always at the expected value, coincident with the nominal electron incidence energy of 4 keV.

Fig. 5 shows the spectral region involving the O-Kα peak for different exposure times. The peak intensity clearly increases for longer times, except for the spectrum corresponding to 307 s, which exhibits a similar O-Kα peak as the spectrum collected during 207 s, suggesting that saturation was reached.

The O-Kα peak maximum values, normalized to account for beam fluctuation and corrected by bremsstrahlung atomic number dependence, as explained in the previous section, are plotted as a function of the exposure time in Fig. 6. As can be seen, the corrosion process takes place at a higher rate during the first seconds. On the other hand, above 300 s, no change can be observed by inspection of the O-Kα peak intensity at 4 keV electron excitation. A comparison of Fig. 6 with the simulations plotted in Fig. 2 suggests that the two abscissa variables, LiOH depth and exposure time, are monotonically related. Each experimental point plotted in Fig. 6 presents two error bars: the vertical one corresponds to the standard deviation arising from averaging five spectra taken at different sample regions, and the horizontal bar is related to the uncertainty in the determination of the exposure time to air, whose main contribution is associated with the number of times that the sample is introduced into the SEM chamber. Regarding the vertical error bar, it increases along the first 100 s and then decreases markedly. This behavior can be understood bearing in mind the SEM images showed in Fig. 4: initially, the preferential nucleation of LiOH around the material defects influences systematically the X-ray spectra despite they were measured at different sample regions chosen randomly. On the other hand, once a mostly uniform LiOH film is formed, the choice of the sample region is not so critical.

We turn to analyze the previous results in the light of the results available in the literature for the present system. The properties and kinetic behavior of corrosion layers formed on Li through the exposure to gases present in air has been reviewed by Phillips and Tanski [3]. These authors pointed out that water diffusion plays an essential role in the formation of these corrosion layers. Additionally, two articles discussed by Phillips and Tanski are particularly relevant to analyze the present results. In a very early work, Deal and Svec [17] analyzed the reaction of lithium with water along the temperature range comprised between 320 and 350 K. These studies were performed through the measurement of hydrogen evolution when lithium is brought in contact with water vapor. Upon assumption that LiOH was formed, diffusion of water to the underlying reactive interface was found to be rate determining. Further work by Irvine and Lund [18], using a microbalance and X-ray diffraction, found two slightly different constant rate regimes. One below 170 min at room temperature and another one at longer times. These results were interpreted in terms of the occurrence at short times of a dense layer, close to the metal surface, made of LiOH, and the further growth of lithium hydroxide monohydrate ($LiOH{\cdot}H_2O$) at the outer surfaces of the hydroxide.

Based on the literature results and the present ones, the corrosion reaction can be written as:

$$Li + H_2O \rightarrow LiOH + \frac{1}{2}H_2 \quad (2)$$

the previous reaction actually involves the following electrochemical reactions:

$$Li \rightarrow Li^+ + e^- \quad (3)$$

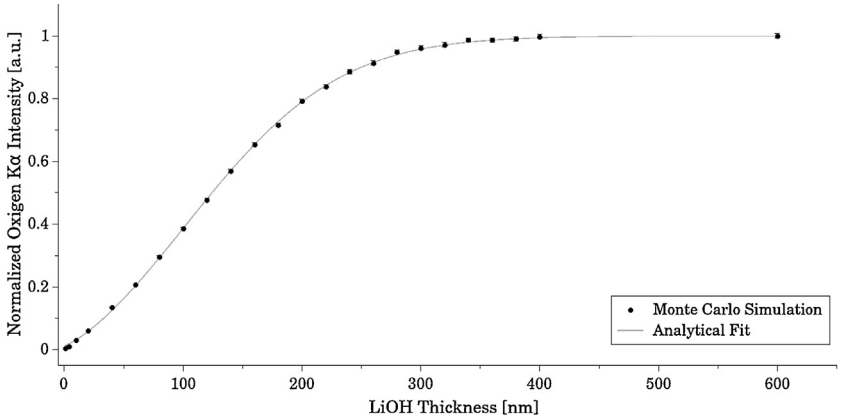

Fig. 2. Characteristic O-Kα intensity for LiOH layers on metallic Li as a function of the layer thickness. Dots: Monte Carlo simulation; solid line: analytical fit using the function described in the text.

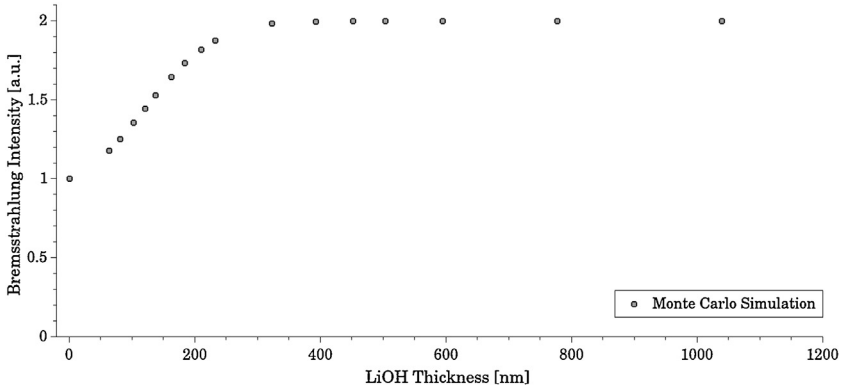

Fig. 3. Bremsstrahlung simulated between 1 and 2 keV for samples composed of a LiOH layer on a thick metallic lithium block. The abscissa corresponds to the LiOH thickness.

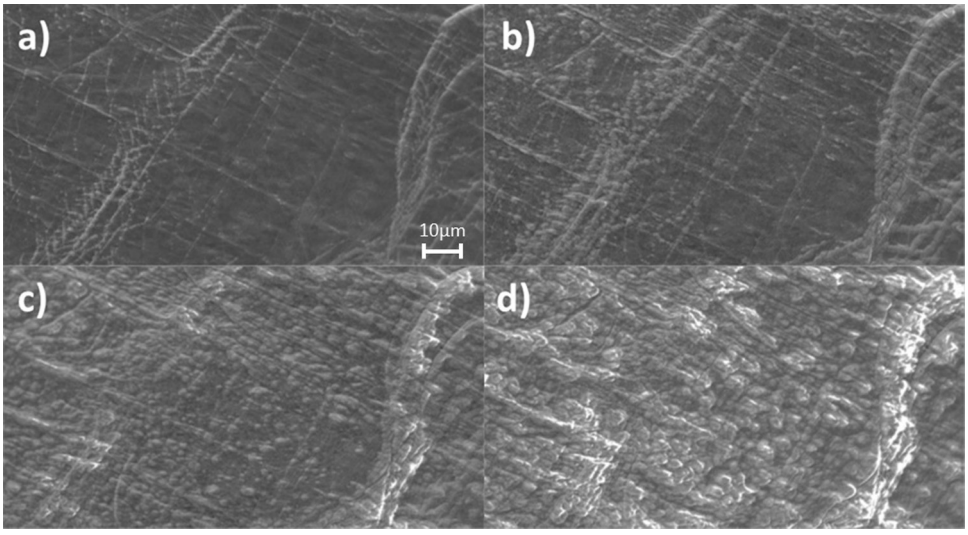

Fig. 4. SEM images taken at the same region of a Li sample after different exposure times to air. (a) 12 s, (b) 52 s, (c) 107 s, (d) 207 s. In all the cases the incidence energy was 4 keV and the magnification was 2000×.

$$e^- + H_2O \rightarrow OH^- + \frac{1}{2}H_2 \quad (4)$$

Two simple mechanisms may be proposed for the previous reactions. On one side, Reaction (3) could take place at the metal/hydroxide interface, while Reaction (4) could take place at the hydroxide/air interface. This mechanism would imply electron transport from the metal to air through the hydroxide by a hopping mechanism, being electron tunneling excluded for the relatively large thicknesses of the LiOH layer analyzed here. Therefore, the only possibility is the conduction through the hydroxide. Corrosion layer growth would thus involve the mobility of Li^+ and/or OH^- ions across the hydroxide as migrating species. The other simple mechanism that can be proposed could be that both Reactions, (3) and (4), would occur at the metal/hydroxide interface, so that

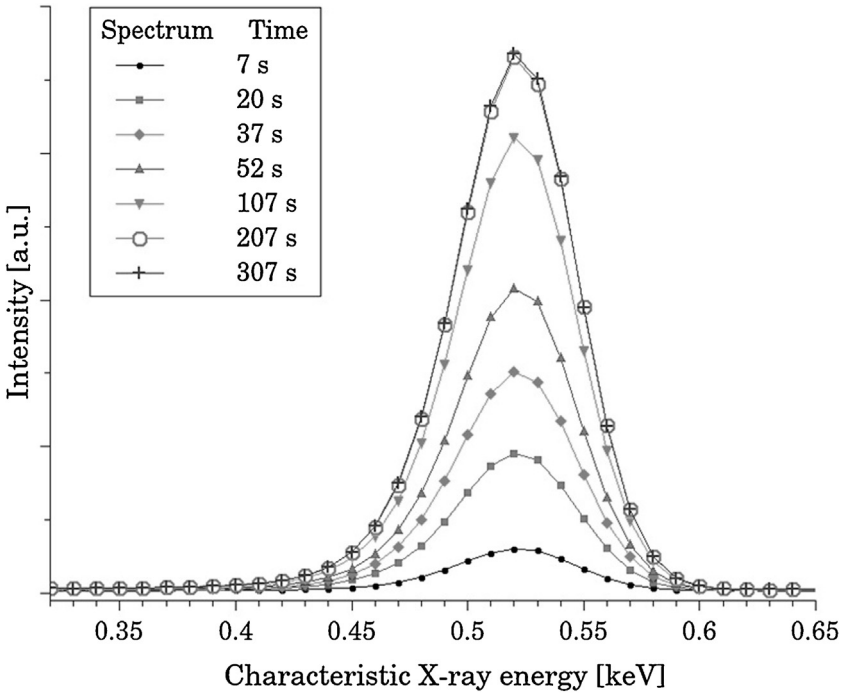

Fig. 5. Spectral region involving the O-Kα peak for different exposure times to air.

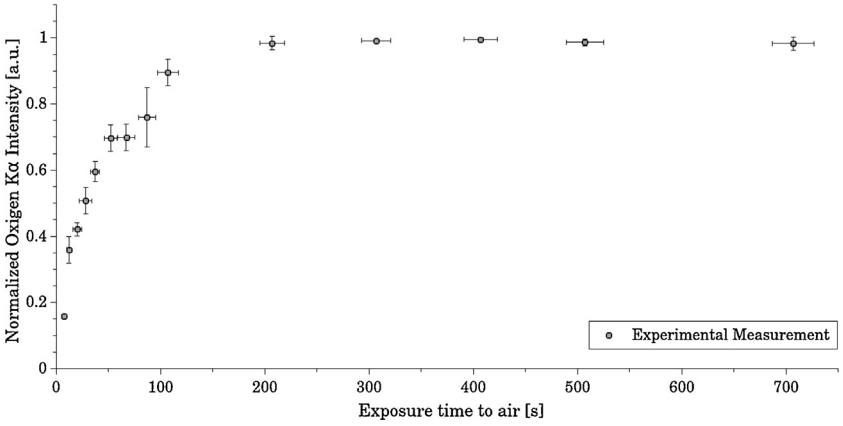

Fig. 6. Normalized O-Kα maximum value as a function of exposure time of a lithium foil to air.

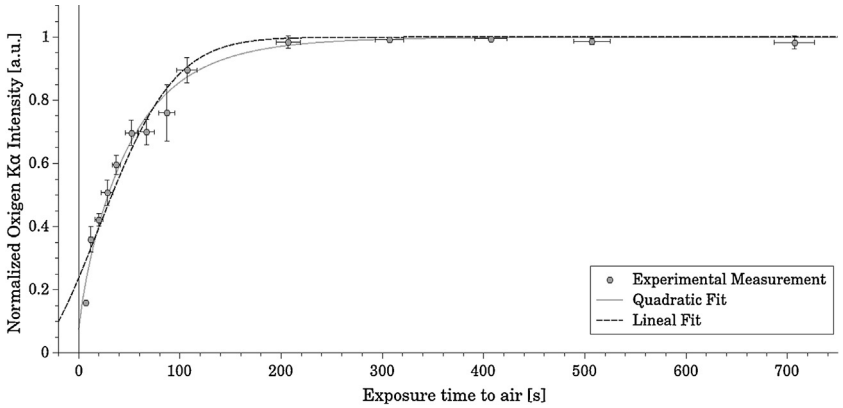

Fig. 7. Normalized O-Kα maximum value as a function of exposure time of a lithium foil to air. Dots: experimental points; dashed black line: analytical fit using function (8), solid grey line: analytical fit using function (7) described in the text.

water should diffuse from air across the hydroxide, reacting at the metal/hydroxide interface.

The first option must be excluded based on data available from the Materials Genome Project [19], where it is found that the band gap for LiOH is typical for an insulator, in any of the two possible crystalline structures. In fact, the band gaps reported are 4.006 eV and 4.002 eV for the tetragonal and orthorombic cases, respectively. Thus, we are left with the second mechanism as operative under the present experimental conditions. This conclusion is in line with the mechanism proposed by Dihn et al. [20] for the growth of thin LiOH films on LiH in high moisture conditions, involving H_2O partial pressure about a few hundred Pascals or more. In order to make quantitative assessments, we will shortly reexamine the work of these authors. According to them, the H_2O flux at the Li/LiOH interface is given by:

$$J = -D_{H_2O}\frac{dC_{H_2O}}{dx} \approx -D_{H_2O}\frac{C_{H_2O}^{surface}}{x} \quad (5)$$

where $D_{H_2}O$ is the diffusion coefficient of water, x is the average film growth thickness, C_{H_2O} and $C_{H_2O}^{surface}$ are the water concentrations at the metal/LiOH and the LiOH/gas interfaces, respectively. On the other hand, the rate of oxide growth is given by:

$$\frac{dx}{dt} = \frac{-J}{C_{OH}^{layer}} \quad (6)$$

where C_{OH}^{layer} is the concentration of OH^- in the LiOH corrosion layer. Combining the two previous equations and integrating, yields:

$$x = \sqrt{2D_{H_2O}\frac{C_{H_2O}^{surface}}{C_{OH}^{layer}}(t + t_0)} \quad (7)$$

which predicts a square-root dependence of the hydroxide thickness with exposure time.

In contrast with this prediction, and using considerably longer exposures times of Li to air, other authors [18] have found a linear dependence of the weight of the Li sample with exposure time, suggesting a linear relationship between thickness and time, say:

$$x = F(t + t_0) \quad (8)$$

In order to check both predictions, the functional forms, (7) and (8), were alternatively introduced into Eq. (1), obtained by Monte Carlo simulations, and fitted to the experimental points according to a least squares procedure. In both cases, an extra parameter t_0 was included to take into account an eventual lithium foil initial aging. Keeping the coefficients A, B and C as fixed parameters, the fitting coefficients obtained were $D = (5.1 \pm 0.4) \times 10^{-12}$ cm^2/s and $t_0 = (1 \pm 2)$ s for Eq. (7), while $F = (1.7 \pm 0.2) \times 10^{-18}$ cm^2/s and $t_0 = (38 \pm 8)$ s were obtained by using Eq. (8). The corresponding plots are shown in Fig. 7, where it can be found that the square-root option yields a better fit than the linear one.

It is important to emphasize that in the case of the square-root functional dependence, the fitted value for the factor $D = 2D_{H_2O} \cdot C_{H_2O}^{surface}/C_{OH}^{layer}$ was $(5.1 \pm 0.4) \times 10^{-12}$ cm^2/s, which is in reasonable good agreement with the value reported by Dihn et al. [15] of the order of 5×10^{-12} cm^2/s for moisture exposure at room temperature with a 18–30% relative humidity.

An additional very important remark can be made regarding the aging parameter t_0: around 40 s was obtained by assuming the linear behavior, whereas no temporal zero shift was found for the rate controlling model, as expected for a fresh lithium foil.

5. Conclusion

First of all, in the present work we have shown that when metallic lithium is exposed to air at room conditions, the only product formed during the first ten minutes is lithium hydroxide (LiOH). Other species such as Li_2CO_3, Li_2O, Li_2O_2 and nitrogen compounds were disregarded due to a detailed analysis based on XPS and EPMA measurements.

The previous discussion shows that the growth kinetics of the hydroxide layer occurring on a Li surface, can be characterized via the measurement of the intensity of the oxygen Kα characteristic line in the X-ray emission spectrum collected with a scanning electron microscope. To the best of our knowledge, this is the first work where studies about the kinetics of lithium corrosion and film grow are reported using EPMA. This technique has the advantage of allowing the study of the reaction layer up to 300 nm, which is a relatively large value.

The experimental results for the normalized O-Kα maximum as a function of the exposure time to air, can be best fitted assuming a square-root dependence of the average film growth thickness with the exposure time, pointing towards the fact that under the present experimental conditions, the growth of the corrosion layer is controlled by water diffusion across the growing Li-OH layer. The calculated diffusive properties agree with estimations reported in literature.

Acknowledgments

Authors are grateful to SeCyT Universidad Nacional de Córdoba, CONICET PIP 11220110100992, Program BID (PICT 2012-2324) and YPF Tecnología (Y-TEC) for financial support. The authors thank the Laboratorio de Microscopía Electrónica y Análisis por Rayos X (LAMARX-UNC) to enable the EPMA-SEM measurements. M. Otero wishes to thank CONICET for a doctoral fellowship.

References

[1] J.-M. Tarascon, M. Armand, Issues and challenges facing rechargeable lithium batteries, Nature 414 (2001) 359–367, http://dx.doi.org/10.1038/35104644.
[2] B. Scrosati, J. Garche, Lithium batteries: status, prospects and future, J. Power Sources 195 (2010) 2419–2430, http://dx.doi.org/10.1016/j.jpowsour.2009.11.048.
[3] J. Phillips, J. Tanski, Structure and kinetics of formation and decomposition of corrosion layers formed on lithium compounds exposed to atmospheric gases, Int. Mater. Rev. 50 (2005) 265–286, http://dx.doi.org/10.1179/174328005X41122.
[4] M. Markowitz, D. Boryta, Lithium metal-gas reactions, J. Chem. Eng. Data 7 (1962) 586–591, http://dx.doi.org/10.1021/je60015a047.
[5] C.R. Tipton, Reactor Handbook, Materials, vol. I, Interscience, New York, 1960.
[6] D.J. David, M.H. Froning, T.N. Wittberg, W.E. Moddeman, Surface reactions of lithium with the environment, Appl. Surf. Sci. 7 (1981) 185–195, http://dx.doi.org/10.1016/0378-5963(81)90108-2.
[7] C. Rigaux, A. Lafort, F. Bodart, Y. Jongen, A. Cambriani, S. Lucas, Analyses of thick lithium coatings deposited by sputter-evaporation and exposed to air, Plasma Process. Polym. 6 (2009) S337–S341, http://dx.doi.org/10.1002/ppap.200930807.
[8] J.R. Hoenigman, R.G. Keil, An XPS study of the adsorption of oxygen and water vapor on clean lithium films, Appl. Surf. Sci. 18 (1984) 207–222, http://dx.doi.org/10.1016/0378-5963(84)90045-x.
[9] R.C. Zeng, L. Sun, Y.F. Zheng, H.Z. Cui, E.H. Han, Corrosion and characterisation of dual phase Mg-Li-Ca alloy in Hank's solution: the influence of microstructural features, Corros. Sci. 79 (2014) 69–82, http://dx.doi.org/10.1016/j.corsci.2013.10.028.
[10] W. Xu, N. Birbilis, G. Sha, Y. Wang, J.E. Daniels, Y. Xiao, et al., A high-specific-strength and corrosion-resistant magnesium alloy, Nat. Mater. 14 (2015) 1229–1236, http://dx.doi.org/10.1038/nmat4435.
[11] R. Younesi, M. Hahlin, F. Björefors, P. Johansson, K. Edström, Li–O_2 battery degradation by lithium peroxide (Li_2O_2): a model study, Chem. Mater. 25 (2013) 77–84, http://dx.doi.org/10.1021/cm303226g.
[12] R. Younesi, P. Norby, T. Vegge, A new look at the stability of dimethyl sulfoxide and acetonitrile in Li-O_2 batteries, ECS Electrochem. Lett. 3 (2014) A15–A18, http://dx.doi.org/10.1149/2.001403eel.

[13] S. Tanaka, M. Taniguchi, H. Tanigawa, XPS and UPS studies on electronic structure of Li_2O, J. Nucl. Mater. 283–287 (2000) 1405–1408, http://dx.doi.org/10.1016/S0022-3115(00)00251-8.
[14] S. Limandri, M. Vasconcellos, R. Hinrichs, J. Trincavelli, Experimental determination of cross sections for K-shell ionization by electron impact for C, O, Al, Si, and Ti, Phys. Rev. A 86 (2012) 042701, http://dx.doi.org/10.1103/PhysRevA.86.042701.
[15] F.A. Filippin, O.E. Linarez Pérez, M.L. Teijelo, R.D. Bonetto, J. Trincavelli, L.B. Avalle, Thickness determination of electrochemical titanium oxide (Ti/TiO_2) formed in $HClO_4$ solutions, Electrochim. Acta 129 (2014) 266–275, http://dx.doi.org/10.1016/j.electacta.2014.02.086.
[16] J.S.F. Salvat, J. Fernández-Varea, PENELOPE- a Code System for Monte Carlo Simulation of Electron and Photon Transport, OECD/NEA Data Bank, Issy-Les-Molineaux, 2008.
[17] B.E. Deal, H.J. Svec, Kinetics of the reaction between lithium and water vapor (1953).
[18] W.R. Irvine, J.a. Lund, The reaction of lithium with water vapor, J. Electrochem. Soc. 110 (1963) 141, http://dx.doi.org/10.1149/1.2425691.
[19] A. Jain, S.P. Ong, G. Hautier, W. Chen, W.D. Richards, S. Dacek, et al., Commentary: The Materials Project: a materials genome approach to accelerating materials innovation, APL Mater. 1 (2013) 011002, http://dx.doi.org/10.1063/1.4812323.
[20] L.N. Dinh, D.M. Grant, M. a. Schildbach, R. a. Smith, W.J. Siekhaus, B. Balazs, et al., Kinetic measurement and prediction of the hydrogen outgassing from the polycrystalline $LiH/Li_2O/LiOH$ system, J. Nucl. Mater. 347 (2005) 31–43, http://dx.doi.org/10.1016/j.jnucmat.2005.06.025.